Current Biology *18*, 255–259, February 26, 2008 DOI 10.1016/j.cub.2008.01.061

Report

Functional and Physical Interaction of Blue- and Red-Light Sensors in *Aspergillus nidulans*

Janina Purschwitz,[1,5] Sylvia Müller,[1,5] Christian Kastner,[1,5] Michelle Schöser,[2] Hubertus Haas,[2] Eduardo A. Espeso,[3] Ali Atoui,[4] Ana M. Calvo,[4] and Reinhard Fischer[1,*]

[1]Department of Applied Microbiology
University of Karlsruhe
Hertzstrasse 16
D-76187 Karlsruhe
Germany

[2]Division of Molecular Biology
Innsbruck Medical University
Fritz-Pregl-Str. 3
A-6020 Innsbruck
Austria

[3]Departmento de Microbiología Molecular
Centro de Investigaciones Biológicas
Ramiro de Maeztu, 9
28040 Madrid
Spain

[4]Department of Biological Science
Northern Illinois University
DeKalb, Illinois 60115

Summary

Light sensing is very important for organisms in all biological kingdoms to adapt to changing environmental conditions. It was discovered recently that plant-like phytochrome is involved in light sensing in the filamentous fungus *Aspergillus nidulans* [1]. Here, we show that phytochrome (FphA) is part of a protein complex containing LreA (WC-1) and LreB (WC-2) [2, 3], two central components of the *Neurospora crassa* blue-light-sensing system. We found that FphA represses sexual development and mycotoxin formation, whereas LreA and LreB stimulate both. Surprisingly, FphA interacted with LreB and with VeA, another regulator involved in light sensing and mycotoxin biosynthesis. LreB also interacted with LreA. All protein interactions occurred in the nucleus, despite cytoplasmic subfractions of the proteins. Whereas the FphA-VeA interaction was dependent on the presence of the linear tetrapyrrole in FphA, the interaction between FphA and LreB was chromophore independent. These results suggest that morphological and physiological differentiations in *A. nidulans* are mediated through a network consisting of FphA, LreA, LreB, and VeA acting in a large protein complex in the nucleus, sensing red and blue light.

Results

A. nidulans Senses Red and Blue Light

In this paper, we studied the light response in *A. nidulans* and found a red- and a blue-light photoresponse when the strain was inoculated as a lawn in a topagar layer (Figure 1, and the Supplemental Experimental Procedures available online). Large numbers of conidiospores were only produced in light, but neither red (light-emitting diode [LED] 680 nm) nor blue (LED 450 nm) light alone induced sporulation to the level of white light (Figure 1B). The combination of both light qualities restored full conidiation. In comparison, both, red and blue light inhibited effectively the sexual cycle. Because development is connected to mycotoxin formation, we investigated which effect different light qualities had on sterigmatocystin (ST) production. A representative result is shown in Figures 1C and 1D. Blue light repressed mycotoxin formation to a similar level as white light did. In comparison, ST production was increased under red-light illumination conditions. Light of 700 nm appeared to be more effective than 680 and 740 nm light. This is in agreement with the fact that the absorption maximum of *A. nidulans* phytochrome lies at 705 nm [1]. These results indicate that *A. nidulans* is able to sense red and blue light. Green light (536 nm) was ineffective (Figure S6). Compared to previous results, it was surprising that blue light stimulated asexual development as much as red light did [4].

To understand the blue-light response at the molecular level, we analyzed the role of *N. crassa* White Collar (WC) homologs in *A. nidulans*. White Collar 1 and 2 are interacting transcription factors characterized from the model fungus *N. crassa* and other fungi, with WC-1 acting as a blue-light sensor. Two genes were identified in *A. nidulans* by colony screening with *wc-1* and *wc-2* probes and named *lreA* and *lreB* (light response) before the genome sequence was available [5]. The open reading frames are disrupted by three introns in the case of *lreA* and one intron in *lreB*. The two deduced proteins share between 34% and 37% identity to the *N. crassa* proteins and comprise similar domain organization as WC-1 and WC-2 do (Figure 2A and Figure S1). The 836 amino acid long LreA protein is characterized by a light-, oxygen-, or voltage-sensitive (LOV) and two PER-ARNT-SIM (PAS) domains, a nuclear localization signal (NLS), and a GATA-type zinc-finger DNA binding domain at the C terminus. The LOV domain harbors the flavin adenine dinucleotide cofactor [2, 3, 6]. PAS domains are involved in protein-protein interaction [7]. LreB is only 417 amino acids long and lacks the LOV domain and one PAS domain in comparison to LreA (Figure 2A and Figure S1). To study the role of the two proteins in *A. nidulans*, we deleted the genes from the genome and analyzed the effect on light-dependent regulation of asexual and sexual development (Figure 2B, and Figure S2). In addition to single mutants, we constructed double and triple mutants with the phytochrome *fphA* and included them into the analysis. Conidiospore production was slightly increased in the Δ*lreA* and Δ*lreB* strains, independent of the presence or absence of light. This suggests a repressing function of LreA and LreB. Conidiation was slightly reduced in Δ*fphA* in the dark and in light in comparison to the wild-type. This suggests that FphA activates asexual development. The fact that the *fphA*-deletion mutant still produced 70% of the number of conidia of the wild-type in light points to the presence of other photoreceptors. Interestingly, double mutation of *lreA* or *lreB* with *fphA* or the triple mutation caused a drastic decrease of the number of conidiospores. However, in the dark and in the light, a basal level of conidiation remained in the absence of the blue- and red-light regulatory proteins (Figure 2B).

*Correspondence: reinhard.fischer@bio.uka.de
[5]These authors contributed equally to this work.

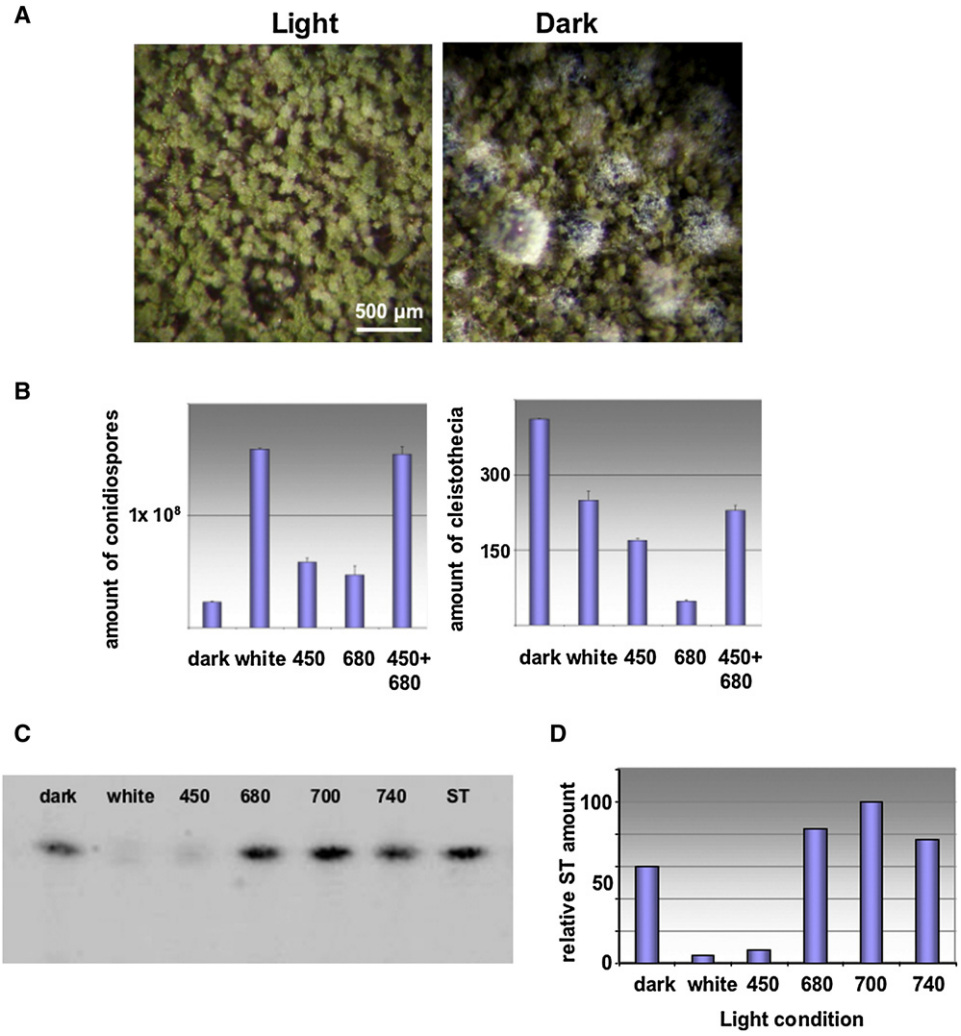

Figure 1. The Light Response in *A. nidulans*

(A) Colonies of FGSCA4 grown under light and dark conditions.

(B) Quantification of conidiospores and cleistothecia formation in the dark, under white, blue (450 nm), red (680 nm), and blue and red light. Conidiospores and cleistothecia were counted as described in the Supplemental Experimental Procedures. The graph shows the average of three independent experiments. Error bars represent the standard deviation.

(C) Sterigmatocystin thin-layer chromatography analysis. Conidia of FGSCA4 were top-agar inoculated (10^7 spores per plate) on minimal medium with 1% glucose and cultured under different light conditions. The wavelengths are indicated as numbers above the lanes. Toxin was extracted after 3 days of incubation.

(D) ST densitometry was carried out with the Scion Image Beta 4.03 software. The normalized ST band intensity values were normalized with respect to the highest intensity considered as 100%. Essentially the same results were obtained in two independent experiments.

The observed phenotypes were recomplemented by the corresponding genes expressed under their native promoters (Figure S5). To test whether the conserved cysteine 276 located in the LOV domain is important for function, we generated a mutant in which this cysteine was replaced by alanine. This mutated version did not complement the triple mutant SJP21.3 (Figure S7).

Sexual development in *A. nidulans* wild-type is the preferred developmental pathway in the dark. Under these conditions, deletion of *lreA* caused a 70% reduction of cleistothecia formation, whereas deletion of *lreB* only caused a 30% reduction (Figure 2B). The Δ*fphA* mutant produced the same number of cleistothecia as the wild-type, and the double and triple mutants behaved similar to the *lreB*-deletion strain. In white light, cleistothecium formation was slightly inhibited in the wild-type and nearly completely lost in *lreA* or *lreB* mutants, suggesting an additive effect of light and the absence of the Lre proteins. The sexual cycle was only slightly reduced in the phytochrome mutant in comparison to the incubation in the dark. The complete loss of cleistothecium formation in the Δ*lreA* or Δ*lreB* strains in light was surprisingly largely suppressed by deletion of *fphA*. Double and triple mutants of *lreA*, *lreB*, and *fphA* incubated in the light produced the same number of cleistothecia as in the dark. This suggests that LreA and LreB act as activators of the sexual cycle and their activity is repressed by light through the action of FphA. These results also show that LreA and LreB serve important functions in the dark. In the absence of positive (LreA, B) and negative (FphA) factors, a basal level of gene induction apparently accounts for the formation of sexual structures.

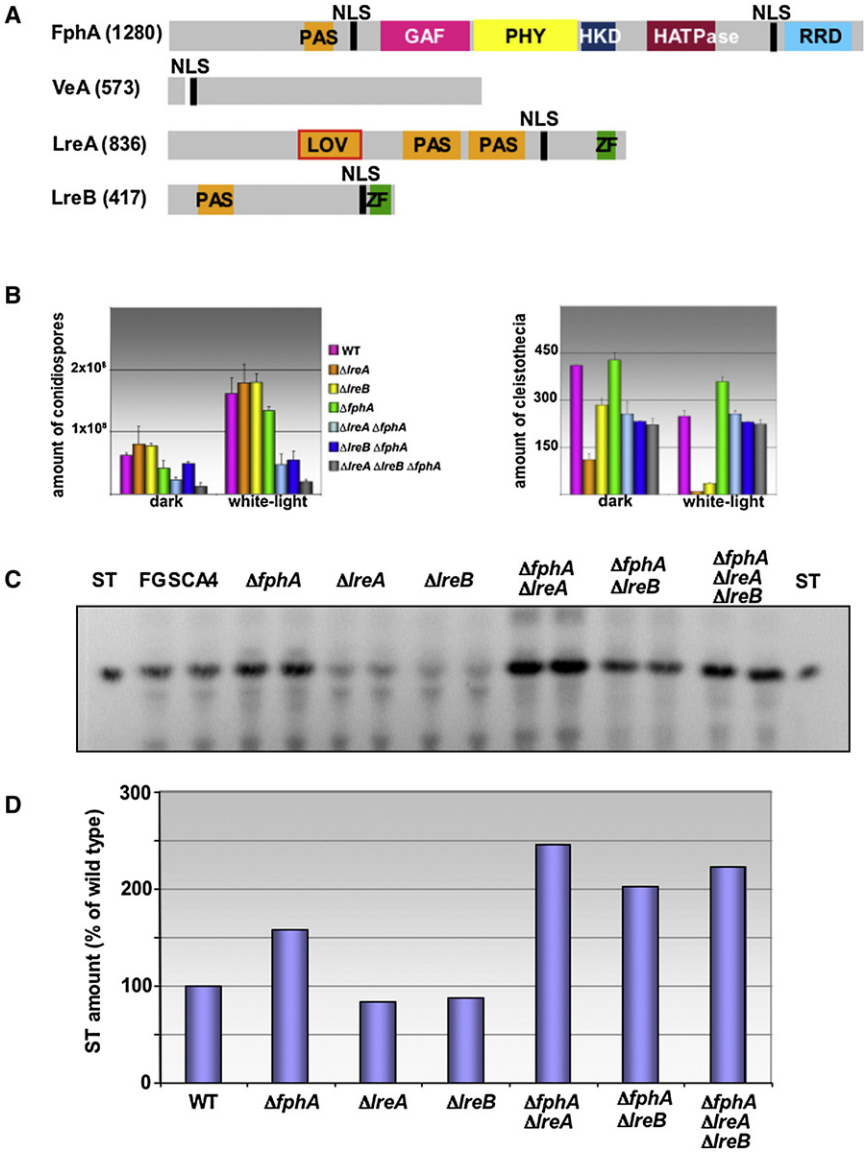

Figure 2. The Role of Phytochrome and White-Collar Proteins in *A. nidulans*

(A) Domain organization of FphA, VeA, LreA, and LreB. Vertical black lines present pat4 nuclear localization sequences, whereas the white vertical line shows a bipartite NLS motif. The following abbreviations are used: PHY, phytochrome domain; GAF, small ligand binding domain; HKD, histidine kinase domain; HATPase, ATPase domain; RRD, response regulator domain; LOV, light, oxygen, voltage domain; PAS, per, arnt, sim domain; ZF, zinc finger.

(B) Effect of deletion of *fphA*, *lreA*, and *lreB* on conidiospore and cleistothecia formation. Quantification was done as described in the Supplemental Experimental Procedures. Error bars represent the standard deviation.

(C and D) Sterigmatocystin formation in light in different mutant strains analyzed by thin layer chromatography (C) and the corresponding quantification (D). So that the low amounts of ST produced in light could be detected, four times more extract was analyzed than in Figure 1C. Essentially the same results were obtained in two independent experiments.

Next, we studied the role of the above characterized light regulators in mycotoxin production. A representative result is shown in Figures 2C and 2D. White and blue light caused a reduction of ST toxin levels compared to those in the dark. The phytochrome mutant strain produced up to 50% more ST and the *lreA* and *lreB* mutants less than the wild-type. The stimulating effect of ST synthesis upon phytochrome deletion was even enhanced in combination with the deletion of the blue-light regulators, LreA and LreB. These results demonstrate a repressing function for phytochrome and an activating function for the WC orthologs and thus a similar regulation as for the formation of cleistothecia.

Interaction of the Blue- and Red-Light Sensing Systems

Because the WC proteins form a complex in *N. crassa*, we asked whether in *A. nidulans* LreA and LreB would interact with each other. First, we studied the localization of LreA and LreB by green fluorescent protein (GFP) fusion. All fusion proteins were shown to be biologically active. LreA and LreB both localized to the nucleus, but LreB also to the cytoplasm (data not shown). To test for physical interaction of LreA and LreB, we used the bimolecular fluorescence complementation (BiFC) assay and cloned the two genes into vectors with the N- or C-terminal yellow fluorescent protein (YFP) halfs, respectively [1]. We transformed the LreA-YFP and LreB-YFP constructs into *A. nidulans* SKV103 and observed fluorescent nuclei (data not shown). The cytoplasm appeared black.

Because the phytochrome and the blue-light-sensing system interacted genetically, we tested whether the proteins would interact physically. By using the BiFC system, we investigated interaction between LreA and FphA and between LreB and FphA. Whereas the first combination did not produce any fluorescent signal in the cell, the second one produced fluorescent nuclei, suggesting LreB-FphA interaction in vivo in the nucleus (Figure 3A). This was surprising because FphA predominantly localized in the cytoplasm, where it also interacts with itself [1]. Our results show that a small fraction of FphA localizes to the nucleus, which was not detected in previous experiments probably because of the high concentration in the cytoplasm [1]. In order to analyze whether light perception of FphA is important for the interaction with LreB, we used a FphA variant in which the chromophore-binding cysteine residue was mutated. Interaction was still detected (data not shown). We also generated FphA derivatives with mutated nuclear localization signals. These mutations did also not affect interaction of FphA with LreB in the nucleus, indicating an alternative nuclear import mechanism for FphA.

The observed interactions of the proteins suggested the existence of a large protein complex, and we wanted to know whether another protein involved in light perception in *A. nidulans*, VeA, would be part of this complex. Therefore, we tested VeA-FphA interaction and the interaction of VeA with LreA or LreB and found that VeA-FphA interaction was positive (data

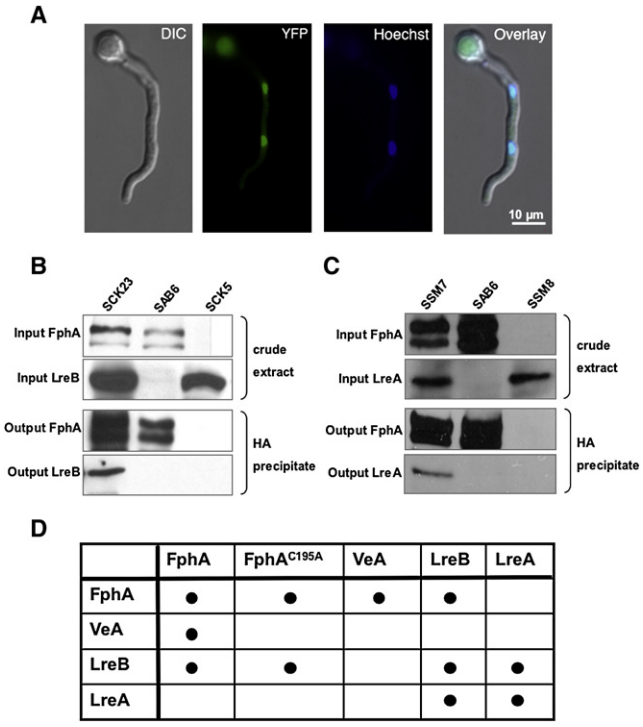

	FphA	FphA^{C195A}	VeA	LreB	LreA
FphA	●	●	●	●	
VeA	●				
LreB	●	●		●	●
LreA				●	●

Figure 3. Protein-Protein Interaction of Polypeptides Involved in the Photoresponse in *A. nidulans*

(A) Interaction between FphA and LreB in the bimolecular fluorescence complementation assay. FphA was fused N-terminally with the N-terminal half of YFP, LreB was fused N-terminally with the C-terminal half of YFP, and both constructs were transformed into *A. nidulans* SKV103. Hyphae are 3–4 μm in diameter.

(B) Verification of the observed FphA-LreB interaction by coimmunoprecipitation.

(C) Interaction between FphA and LreA shown by coimmunoprecipitation.

(D) Summary of the interactions observed in the BiFC system.

not shown). Interestingly, the interaction was again restricted to the nucleus, despite the presence of both proteins in the cytoplasm [1, 8]. No interaction was detected when the chromophore-binding cysteine in FphA was mutated. In order to confirm the data obtained with the BiFC system in vivo, we did coimmunoprecipitation in vitro by using hemagglutinin (HA)- and GFP-tagged protein versions (Figure 3B, Figure S4A). Although there was no evidence for an interaction between FphA and LreA with the BiFC system, we were able to pull down LreA in coimmunoprecipitation experiments (Figures 3C and 3D). This demonstrates that FphA and LreA reside in the same protein complex without direct protein-protein interaction. As further proof for the existence of a large light-sensing protein complex, we precipitated VeA and detected in the pellet fraction LreA and FphA (Figure S4). Assuming that LreA acts as a blue-light sensor, the last result suggests that red- and blue-light perception occur in the same protein complex. For coimmunoprecipitation experiments, the *alcA* promoter-driven constructs were induced with threonine in the culture medium, resulting in strong expression. To reduce the expression level of these proteins, we used glycerol instead of threonine as carbon source. Under these growth conditions, the proteins were not detectable anymore even in the crude cell extract. Phytochrome, VeA, LreA, and LreB were also not detectable when expressed under their natural promoters.

It was shown recently that VeA is largely localized in nuclei when grown in the dark, but VeA presence in the nucleus is decreased when grown in the light [8]. Because VeA itself probably is not able to sense light, we asked whether VeA subcellular localization was dependent on the presence of the phytochrome and found that indeed the decrease of VeA levels in the nucleus was partly dependent on FphA (Figure S3). The fact that nuclear concentration of VeA is prevented by blue light [8] reflects that both red- and blue-light-sensing systems are required for effective nuclear localization.

Discussion

Light sensing is very important for organisms in all kingdoms to adapt to changing environmental conditions and is mediated only by a few photoreceptor molecules, two of which are phytochromes, for red light, and flavoproteins, for blue light. Phytochromes were thought to be confined to photosynthetic organisms including cyanobacteria [9–11] but have been recently discovered in heterotrophic eubacteria and in fungi [1, 12, 13]. Phytochrome as well as blue-light sensors are absent from *Saccharomyces cerevisiae* and *Schizosaccharomyces pombe*. Phytochrome, FphA, and a fungal-specific protein, VeA, have been described as important components of the light response in *A. nidulans* [1, 4]. Certain mutant strains of *A. nidulans* were reported to react on blue light (436 nm), in addition to red light, suggesting the presence of a blue-light-sensing system, as well [14]. In addition to the morphogenetic decisions, light reduces the formation of the *A. nidulans* mycotoxin ST. This regulation involves also the *veA* gene, suggesting common regulatory pathways [15].

The blue-light response is best studied in *Neurospora crassa* but has been recently studied also in other fungi [2, 3, 13, 16–18]. Two main players are WC-1 and WC-2, which are both transcription factors. WC-1 contains flavin as the light-receptor molecule [2, 3]. Both proteins are nuclear localized, but a fraction of WC-2 was also detected in the cytoplasm, and both undergo light-dependent phosphorylation. Neither light nor phosphorylation had an effect on the localization [19]. Besides the well-studied blue-light response in *N. crassa*, a red-light response has been described several decades ago as potentiation of X-ray-induced genetic damage by far-red light. This effect was reversible when the culture was illuminated with red light after far-red-light exposure and thus resembled a phytochrome response [20]. Indeed, two phytochrome homologs were identified recently in the genome, but deletion of the phytochromes did not cause any obvious developmental phenotype [16]. Genetic damage was not analyzed in this publication.

We show in this paper that morphological and physiological differentiation in *A. nidulans* is regulated through an interplay between two light-sensing systems, which involves direct protein-protein interaction (Figure 3). This raises the question of how common such an interaction would be, given that in many fungal genomes, photoreceptors for several light qualities were found. In *N. crassa*, the white-collar protein complex was purified, and WC-1 and WC-2 were identified in a ratio of 1:1 [2]. This depicts that in *N. crassa*, which contains two phytochromes and also a VeA ortholog, only blue-light perception is mediated through the protein complex. Similar to the results obtained for *N. crassa*, deletion of the phytochrome gene in *Cryptococcus neoformans* did not exhibit a phenotype [18]. On the other hand, the function of the WC proteins as blue-light receptors is well conserved during fungal evolution [17, 18].

There are examples that fungi respond to blue and to red light [21], but a functional and physical interplay between the two light-sensing systems has not been reported yet in any other fungus.

After the discovery of the interplay between the red- and the blue-light response in *A. nidulans*, it will be the challenge for future research to identify pathway-specific transcription factors, which convert the light response into differential gene expression. These transcription factors are likely to be interaction partners of the response regulator of FphA (Figure 2A). Whether the changes of the activities of VeA, LreA, and/or LreB are due to modulations of the protein activities or due to changes of the protein levels is another important question to be solved for better understanding photosensory responses. Our results suggest that photosensing in fungi appears not only to share crucial proteins such as phytochrome with higher plants, but also that integration of different light qualities is an ancient process conserved from bacteria [22] to fungi to plants [23].

Supplemental Data

Experimental Procedures, seven figures, and two tables are available at http://www.current-biology.com/cgi/content/full/18/4/255/DC1/.

Acknowledgments

We thank Suzanne Stinnett and Tamir Shelo for technical support. This work was supported by the Deutsche Forschungsgemeinschaft (DFG), the Max-Planck-Institute for terrestrial Microbiology (Marburg), the special programme "Lebensmittel und Gesundheit" from the ministry of Baden-Württemberg, the Spanish Ministerio de Educación y Ciencia, grant BFU2006-04185, and the Northern Illinois University.

Received: July 6, 2007
Revised: January 8, 2008
Accepted: January 9, 2008
Published online: February 21, 2008

References

1. Blumenstein, A., Vienken, K., Tasler, R., Purschwitz, J., Veith, D., Frankenberg-Dinkel, N., and Fischer, R. (2005). The *Aspergillus nidulans* phytochrome FphA represses sexual development in red light. Curr. Biol. *15*, 1833–1838.
2. He, Q., Cheng, P., Yang, Y., Wang, L., Gardner, K.H., and Liu, Y. (2002). White collar-1, a DNA binding transcription factor and a light sensor. Science *297*, 840–843.
3. Froehlich, A.C., Liu, Y., Loros, J.J., and Dunlap, J.C. (2002). White collar-1, a circadian blue light photoreceptor, binding to the frequency promoter. Science *297*, 815–819.
4. Mooney, J.L., and Yager, L.N. (1990). Light is required for conidiation in *Aspergillus nidulans*. Genes Dev. *4*, 1473–1482.
5. Galagan, J.E., Calvo, S.E., Cuomo, C., Ma, L.-J., Wortman, J.R., Batzoglou, S., Lee, S.-I., Bastürkmen, M., Spevak, C.C., Clutterbuck, J., et al. (2005). Sequencing of *Aspergillus nidulans* and comparative analysis with *A. fumigatus* and *A. oryzae*. Nature *438*, 1105–1115.
6. Crosson, S., Rajagopal, S., and Moffat, K. (2003). The LOV domain family: Photoresponsive signaling modules coupled to diverse output domains. Biochemistry *42*, 2–10.
7. Cheng, P., Yang, Y., Gardner, K.H., and Liu, Y. (2002). PAS domain-mediated WC-1/WC-2 interaction is essential for maintaining the steady state level of WC-1 and the function of both proteins in circadian clock and light responses of *Neurospora*. Mol. Cell. Biol. *22*, 517–524.
8. Stinnett, S.M., Espeso, E.A., Cobeno, L., Araujo-Bazan, L., and Calvo, A.M. (2007). *Aspergillus nidulans* VeA subcellular localization is dependent on the importin alpha carrier and on light. Mol. Microbiol. *63*, 242–255.
9. Kehoe, D.M., and Grossman, A.R. (1996). Similarity of a chromatic adaptation sensor to phytochrome and ethylene receptors. Science *273*, 1409–1412.
10. Yeh, K.-C., Wu, S.-H., Murphy, J.T., and Lagarias, J.C. (1997). A cyanobacterial phytochrome two-component light sensory system. Science *277*, 1505–1508.
11. Giraud, E., Fardoux, J., Fourrier, N., Hannibal, L., Genty, B., Bouyer, P., Dreyfus, B., and Vermeglio, A. (2002). Bacteriophytochrome controls photosystem synthesis in anoxygenic bacteria. Nature *417*, 202–205.
12. Bhoo, S.-H., Davis, S.J., Walker, J., Karniol, B., and Vierstra, R.D. (2001). Bacteriophytochromes are photochromic histidine kinases using a biliverdin chromophore. Nature *414*, 776–779.
13. Purschwitz, J., Müller, S., Kastner, C., and Fischer, R. (2006). Seeing the rainbow: Light sensing in fungi. Curr. Opin. Microbiol. *9*, 566–571.
14. Yager, L.N., Lee, H.O., Nagle, D.L., and Zimmermann, J.E. (1998). Analysis of *fluG* mutations that affect light-dependent conidiation in *Aspergillus nidulans*. Genetics *149*, 1777–1786.
15. Kato, N., Brooks, W., and Calvo, A.M. (2003). The expression of sterigmatocystin and penicillin genes in *Aspergillus nidulans* is controlled by *veA*, a gene required for sexual development. Eukaryot. Cell *2*, 1178–1186.
16. Froehlich, A.C., Noh, B., Vierstra, R.D., Loros, J., and Dunlap, J.C. (2005). Genetic and molecular analysis of phytochromes from the filamentous fungus *Neurospora crassa*. Eukaryot. Cell *4*, 2140–2152.
17. Idnurm, A., Rodriguez-Romero, J., Corrochano, L.M., Sanz, C., Iturriaga, E.A., Eslava, A.P., and Heitman, J. (2006). The Phycomyces *madA* gene encodes a blue-light photoreceptor for phototropism and other light responses. Proc. Natl. Acad. Sci. USA *103*, 4546–4551.
18. Idnurm, A., and Heitman, J. (2005). Light controls growth and development via a conserved pathway in the fungal kingdom. PLoS Biol. *3*, 615–626.
19. Schwerdtfeger, C., and Linden, H. (2000). Localization and light-dependent phosphorylation of white collar 1 and 2, the two central components of blue light signaling in *Neurospora crassa*. Eur. J. Biochem. *267*, 414–421.
20. Klein, R.M., and Klein, D.T. (1962). Interaction of ionizing and visible radiation in mutation induction in *Neurospora crassa*. Am. J. Bot. *49*, 870–874.
21. Lee, K., Singh, P., Chung, W.C., Ash, J., Kim, T.S., Hang, L., and Park, S. (2006). Light regulation of asexual development in the rice blast fungus, *Magnaporthe oryzae*. Fungal Genet. Biol. *43*, 694–706.
22. Montgomery, B.L. (2007). Sensing the light: Photoreceptive systems and signal transduction in cyanobacteria. Mol. Microbiol. *64*, 16–27.
23. Jiao, Y., Lau, O.S., and Deng, X.W. (2007). Ligth-regulated transcriptional networks in higher plants. Nat. Rev. Genet. *8*, 217–230.

Supplemental Data

Functional and Physical Interaction of Blue- and Red-Light Sensors in *Aspergillus nidulans*

Janina Purschwitz, Sylvia Müller, Christian Kastner, Michelle Schöser, Hubertus Haas, Eduardo A. Espeso, Ali Atoui, Ana M. Calvo, and Reinhard Fischer

Supplemental Experimental Procedures

Strains, Culture Conditions and Plasmids

Supplemented minimal media for *A. nidulans* were prepared as previously described, and standard strain construction procedures were used [S1]. A list of *A. nidulans* strains used in this study is given in Table S1. Standard DNA transformation procedures were used for *A. nidulans* [S2] and *Escherichia coli* [S3]. For polymerase chain reaction (PCR) experiments, standard protocols were applied with a rapid cycler (Biometra, Göttingen). Genomic DNA for PCR was extracted with the DNeasy plant mini kit (QIAGEN, Hilden, Germany).

The open reading frames (ORFs) of *veA*, *lreA*, and *lreB* were amplified with the following primers: VeA_AscI_for_new, 5′-GGCGCGCCTATGGCTACACT TGCA-3′; VeA_PacI_rev, 5′-TTAATTAAGTGCCCAGAGCCCGGTT-3′; LreA_A scI_for, 5′-GGCGCGCCTATGGCCAATCGAGAT-3′; LreA_PacI_rev, 5′-TTA ATTAACTGACCTCTATACCCCTGCG-3′; LreB_AscI_for, 5′-GGCGCGCCTAT GGATCCCACCCA-3′; and LreB_PacI_rev, 5′-TTAATTAAGAAAGATGGGTAG GCGAGGTATCG-3′. PCR products were cloned into pCR2.1-TOPO vector (Invitrogen, Leed, NL). Afterward, the genes were inserted into pMCB17apx with AscI and PacI restriction sites. For the BiFC assays, we exchanged GFP in pMCB17apx with the C and N terminus of YFP, respectively [S4].

Isolation of *lreA* and *lreB*

A *lreA*-specific 77 bp radioactive-labeled probe for screening of *lreA*-containing cosmids was generated by PCR (OWC2, 5′-AAYACNCCNGAP TGGMG-3′; and OWC3, 5′-AGYTGYTTNGCCCANC-3′). The identified cosmid W16/G02 was digested with EcoRI, and the resulting 4.3 kb fragment was cloned into pBS-KS, resulting in pL1E5, which was sequenced. The intron-exon borders were identified by PCR amplification of complementary DNA (cDNA) with the primers OW1 (5′-CAGCTTTGAACTACGAC-3′) and OW8 (5′-CACCCTCAAATGACAAT-3′). After isolation of the PCR fragment, it was cloned into pGEM-T (Promega) and sequenced. The 3′ cDNA end of *lreA* was amplified by 3′ RACE with primers OW9 (5′-TGTACTCACCTATCCA G-3′) and d(T)17, subcloned into pGEM-T, and sequenced.

The *lreB* gene was isolated by colony screening of a FGSC pWE15 cosmid library [S5]. A 60 bp radioactive-labeled probe was used, generated by PCR (OWC2, 5′-AAYACNCCNGAPTGG(A,C)G-3′; and GATA2, 5′-ARNCCRCANG CRTTRCA-3′). The identified cosmid W21/A03 was digested with EcoRI, and the resulting 6 kb fragment was cloned into pBS-KS, resulting in pLREB65, which was sequenced. The intron-exon borders were identified by PCR amplification of cDNA with the primers OLR7 (5′-TAAATGCGCGGACTGT GG-3′) and LRE1 (5′-AGCAAGGCAACTGACAAC-3′). After isolation of the PCR fragment, it was cloned into pGEM-T and sequenced.

Construction of *lreA*- and *lreB*-Deletion Strains

lreA-*Deletion Vector*

A 2.8 kb PstI-BamHI fragment was generated from pILJ16, including the coding region of the *argB* gene. With T4 polymerase, the BamHI restriction site was refilled. The *lreA*-containing plasmid pL1E5 was digested with SnaBI. After blunt-end generation, a partial digest with NsiI was performed. The PstI- and BamHI-restricted *argB* fragment was inserted into the 5.2 kb pL1E5 vector, resulting in pLREA/KO. In this vector, the open reading frame, except the first 880 nucleotides, was exchanged by the *argB* gene.

lreB-*Deletion Vector*

The *lreB*-containing vector pLREB65 was digested with SfuI and BclI and the SfuI site refilled with Klenow. These digests were performed in a *dam*$^{-}$ background for the assurance that the BclI site was not protected by a methyl group. The PstI-and BamHI-restricted *argB* fragment (2.8 kb) was inserted into the 6.5 kb SfuI-BvlI pLREB65 vector, resulting in pLREB/KO. The strain WG355 was transformed with EcoRI fragments of pLREA/KO and pLREB/KO. Medium without arginine was used for the selection of transformed clones. The resultant knockout strains were crossed with UC9 so that *ve*+ strains could be obtained.

Southern-Blot Analysis of *lreA*-Deletion Strains

Genomic DNA was isolated from transformants, EcoRI digested, separated by electrophoresis, and blotted onto a nylon membrane (HybondTM N, 0.45 μm, Amersham), which was hybridized with a digoxigenin-labeled DNA probe, amplified by PCR. With the use of the 3′ border as a probe (OW7, 5′-TTCCCGTTCGGCTTTGA-3′; and OW32, 5′-ACTGGGCTCATTCTA AC-3′), the wild-type showed a 4.3 kb signal, whereas the knockout displayed a 5 kb signal. The integration event was confirmed witha second probe (OW10, 5′-TTCCGCTTTCGTCTCCG-3′; and OW5, 5′-CGAGAACACA GATGACC-3′) after EcoRI digest, resulting in a 4.3 kb signal in case of wild-type strains. In knockout strains, this signal was absent. See Figure S2.

Southern-Blot Analysis of *lreB*-Deletion Strains

Genomic DNA was isolated and digested with EcoRI. With the use of probe 1 (OLR5, 5′-AGCGAGTCACAGTTACCC-3′; and OLR6R, 5′- GCCTTTTCCTGG ACTCAT-3′) indicated in Figure S2, an 8 kb signal was observed in wild-type, whereas the deletion strains showed no signal. The integration event was confirmed by a second Southern blot with probe 2 (OARG1, 5′-TTCGCTC CGTACTCAAG-3′; and OARG2, 5′-GAGTAGCGACAGCAATG-3′), which binds to the *argB* cassette. As expected, in wild-type strains, a single 9 kb signal was obtained, whereas in the knockout strains, a double band of 9 and 8.4 kb occurred. See Figure S2.

Cultivation and Quantification of Conidiospores and Cleistothecia

Strains were inoculated in 5 ml topagar (0.8%) with a spore density of 2.5 × 10^5 spores. Topagar was distributed evenly on minimal medium (MM) plates and overlaid with liquid medium. Samples were incubated for 20 hr at 37°C to gain developmental competence. Then liquid medium was removed carefully and incubated for further 24 hr for the quantification of asexual spores or for 5 days for the quantification of cleistothecia. The number of conidiospores or cleistothecia was quantified from an agar core of 0.8 cm diameter. So that the conidiospores could be counted, the agar core was incubated for 10 min in a rotator with 500 μl water containing 1% Tween 20. As light sources, we used LEDs for red light (680 nm and 740nm) and blue light (450 nm) (Roithner, Vienna, Austria). For illumination with green light, a LED bulb with a maximum at 536 nm (Electronic, Hirschau, Germany) was used. The fluence rates were about 25 μE/m^2s for LEDs and 30 μE/m^2s for white light.

Mutagenesis of the Nuclear Localization Signals of FphA

Site-directed mutant ΔRRRK and ΔRPKK were constructed with the site-directed mutagenesis kit (Stratagene) with pJP4 as template. The following primers were used: ΔRRRK, 5′-AGCGCGACGCAGGAC-3′ (fwd) and ΔRP KK, 5′-AGTCTGAGCTTCGCTTTCAC-3′; the second primer was the complement of the displayed one, respectively.

Mutagenesis of the Putative Chromophore Binding Site of LreA

A C276A mutant was constructed with the site-directed mutagenesis kit (Stratagene) with primer LreA C276A for 5′-GTTGGGCGCAATGCACGCTTC CTTC-3′ (fwd) and the complementary second primer. Plasmid pJP33 was used as template.

Tagging of Proteins with GFP or Split YFP

The *veA*::*gfp* transformation cassette, generated as described in [S6], was transformed into *A. nidulans* RSMS2.3A (Δ*fphA::argB, pyroA4, pyrG89, veA*+) for the obtainment of TEEAMC8 (Δ*fphA::argB, pyroA4, pyrG89, veA*+::GFP) (Figure S3). RSMS2.3A was obtained by meiotic recombination between SAB1 (*pyrG89,* Δ*argB::trpC*Δ*B, pyroA4,* Δ*fphA::argB, veA1*) and WIM 126 (*pabaA1, yA2; veA*+). Strain TRMD3.4.17 (*pyroA4; veA*+*::gfp::pyrG*$^{A.fumigatus}$, [S6]) was used as control.

pJP52 is derived from pJP7.1. The *fphA* mutant C195A was constructed with the site-directed mutagenesis kit (Stratagene) with primer 5′-CGTTGAC TCTTTCAAAGCCGCCGAAGACGAGC-3′ (fwd). The second primer was the complement to the displayed primer. YN and YC were released with KpnI

and AscI from pDV6 (YC) [S4] and used for the replacement of GFP2-5 in pJP7.1 and the production of plasmid pJP52 (YC-FphAC195A).

Protein Extracts, Immunoprecipitation, and Western Blotting

For induction of the *alcA* promoter, *A. nidulans* cultures were shaken in minimal medium containing 2% threonine and 0.2% glucose for 24–28 hr. The mycelium was harvested by filtration through Miracloth (Calbiochem, Heidelberg), dried by pressing between paper towels, and immediately frozen in liquid nitrogen. After the mycelium was ground in liquid nitrogen, the material was resuspended in protein extraction buffer (20 mM Tris-HCl [pH 8], 0.05% Triton X-100, 150 mM NaCl) supplemented with protease inhibitors (1 mM phenylmethylsulfonyl fluoride, 10 μM leupeptin, 1 μM pepstatin). Protein extracts were clarified twice by centrifugation (Eppendorf Centrifuge 5403; Eppendorf, Hamburg) at 13,000 rpm at 4°C for 10 min. For immunoprecipitation (IP) experiments, 1 ml of the protein extract (~10 mg protein/ml) was adjusted to 300 mM NaCl with 5 M NaCl solution and subsequently incubated with 5 μl monoclonal antibody HA.11 (clone 16B12; Hiss Diagnostics, Freiburg) for at least 1 hr at 10°C. Fifty microliters of 50% protein G agarose (Roche, Mannheim) were added to a volume of 1 ml protein extract, and incubation was continued for at least 3 hr. Agarose beads were pelleted by centrifugation in Eppendorf Centrifuge at 15,000 rpm at 4°C for 30 s. The pellet was washed two times with protein extraction buffer. Proteins were eluted by boiling in sodium dodecyl sulfate sample buffer for 5 min. Aliquots were subjected to sodium dodecyl sulfate polyacrylamide gel electrophoresis and Western-blot analysis (WB). For WB, a monoclonal antibody raised against the hemagglutinin (HA) epitope (dilution 1:1000), or against the green fluorescent protein (Product G 1544; Sigma-Aldrich, München; dilution 1:4000) was used. Nitrocellulose membranes from Schleicher and Schuell, Dassel, were used.

BiFC System and Epifluorescence Microscopy

Two candidate genes were fused with the C or N terminus of YFP, respectively. These plasmids, derived from pMCB17apx, were transformed into *A. nidulans* strain SKV103. Germlings were grown for 24 hr at room temperature (RT) in liquid MM with glycerol for the induction of the *alcA*-promoter, which controls the transcription of the constructs. For the analysis of older hyphae, the fungus was grown in small Petri dishes with glass bottom (WillCo Wells, Amsterdam, The Netherlands). The mycelium was analyzed with a Zeiss AxioImagerZ.1 (Jena, Germany) with an 63 Plan-ApoChromat Objective with YFP filtersets. Pictures were taken with the Zeiss AxioCamMR. An ORCA-ER digital camera (Hamamatsu) coupled to a NIKON E-600 microscope was also used.

Thin-Layer Chromatography

The production of sterigmatocystin was monitored via thin-layer chromatography. The strains SJP1 (Δ*fphA*), LA (Δ*lreA*), LB (Δ*lreB*), SJP13 (Δ*fphA*, Δ*lreB*), SJP15 (Δ*fphA*, Δ*lreA*), SJP21 (Δ*fphA*, Δ*lreA*, Δ*lreB*), and the wild-type FGSCA4 were inoculated on supplemented minimal-medium plates (1.5% agar) with a spore density of 10^7 and incubated under different light conditions at 30°C. After 3 days, four cores of 18 mm in diameter were collected and extracted by the addition of 7 ml chloroform, two consecutive times. The extracts were combined, dried in a nitrogen stream, and resolved in 500 μl acetonitrile. Ten to forty microliters of each extract were spotted on TLC plates (Silica gel 60, 10 × 20 cm, Merck, Darmstadt, Germany). The samples were fractionated with toluene, ethyl acetate, and acetic acid 80:10:10 (vol/vol/vol) as a solvent system. For the intensification of fluorescence upon exposure to eltraviolent (UV) light (365 nm), the plates were sprayed with water-free aluminum chloride (15% in ethanol) and subsequently baked for 10 min at 80°C. Sterigmatocystin (Sigma) was used as a standard. The band intensity was quantified with Scion Image Beta 4.03 software.

Supplemental References

S1. Käfer, E. (1977). Meiotic and mitotic recombination in *Aspergillus* and its chromosomal aberrations. Adv. Genet. *19*, 33–131.

S2. Yelton, M.M., Hamer, J.E., and Timberlake, W.E. (1984). Transformation of *Aspergillus nidulans* by using a *trpC* plasmid. Proc. Natl. Acad. Sci. USA *81*, 1470–1474.

S3. Sambrook, J., and Russel, D.W. (1999). Molecular Cloning: A Laboratory Manual (Cold Spring Harbor, New York: Cold Spring Harbor Laboratory Press).

S4. Blumenstein, A., Vienken, K., Tasler, R., Purschwitz, J., Veith, D., Frankenberg-Dinkel, N., and Fischer, R. (2005). The *Aspergillus nidulans* phytochrome FphA represses sexual development in red light. Curr. Biol. *15*, 1833–1838.

S5. Brody, H., Griffith, J., Cuticchia, A.J., Arnold, J., and Timberlake, W.E. (1991). Chromosome-specific recombinant DNA libraries from the fungus *Aspergillus nidulans.* Nucleic Acids Res. *19*, 3105–3109.

S6. Stinnett, S.M., Espeso, E.A., Cobeno, L., Araujo-Bazan, L., and Calvo, A.M. (2007). *Aspergillus nidulans* VeA subcellular localization is dependent on the importin alpha carrier and on light. Mol. Microbiol. *63*, 242–255.

S7. Waring, R.B., May, G.S., and Morris, N.R. (1989). Characterization of an inducible expression system in *Aspergillus nidulans* using *alcA* and tubulin coding genes. Gene *79*, 119–130.

S8. Karos, M., and Fischer, R. (1999). Molecular characterization of HymA, an evolutionarily highly conserved and highly expressed protein of *Aspergillus nidulans.* Mol. Genet. Genomics *260*, 510–521.

S9. Brakhage, A.A., Browne, P., and Turner, G. (1992). Regulation of *Aspergillus nidulans* penicillin biosynthesis and penicillin biosynthesis genes *acvA* and *ipnA* by glucose. J. Bacteriol. *174*, 3789–3799.

S10. Gems, D., Johnstone, I.L., and Clutterbuck, A.J. (1991). An autonomously replicating plasmid transforms *Aspergillus nidulans* at high frequency. Gene *98*, 61–67.

S11. Osmani, A.H., May, G.S., and Osmani, S.A. (1999). The extremely conserved *pyroA* gene of *Aspergillus nidulans* is required for pyridoxine synthesis and is required indirectly for the resistance to photosensitizers. J. Biol. Chem. *274*, 23565–23569.

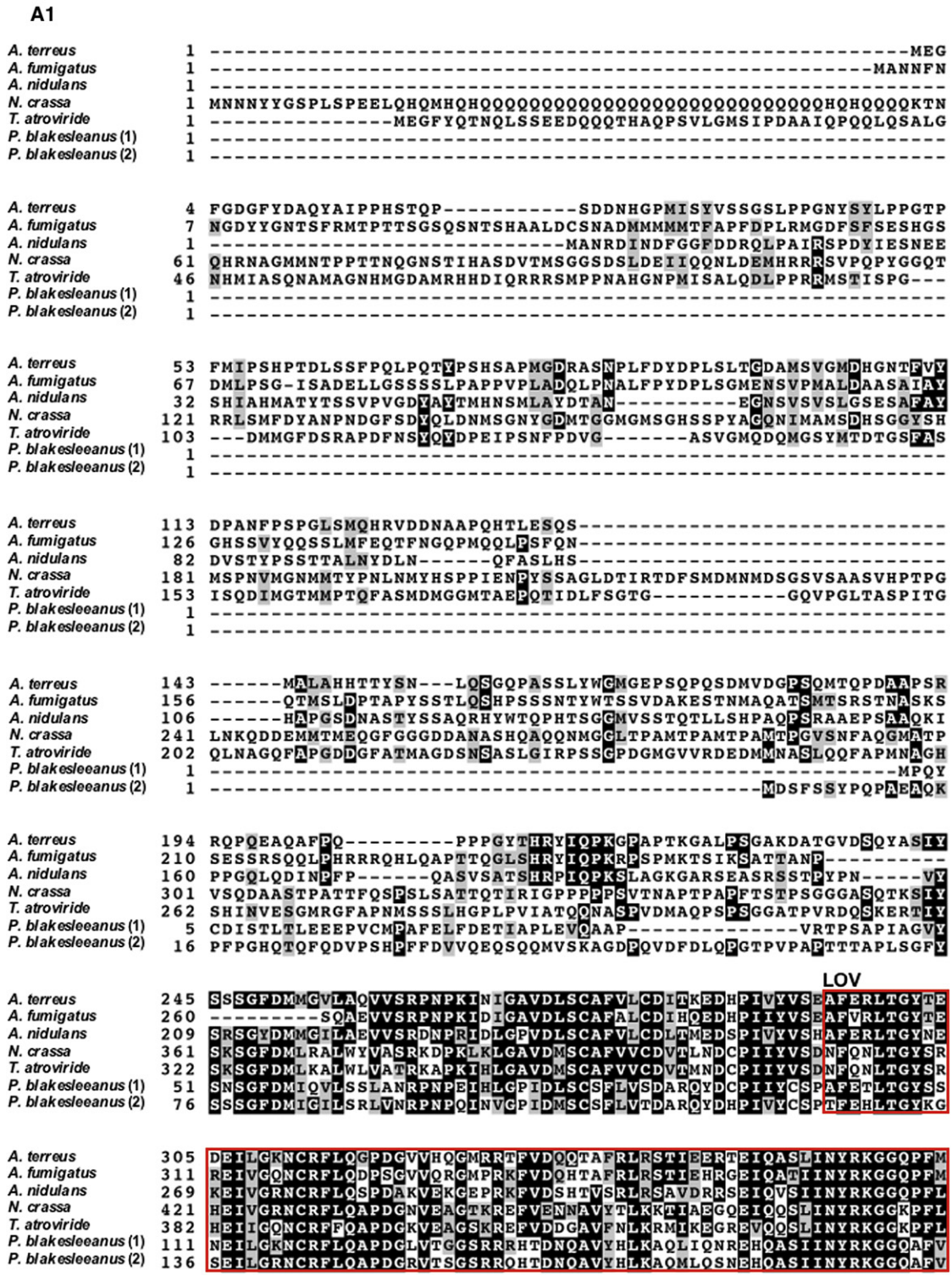

Figure S1. Sequence Alignment of LreA and LreB with WC Proteins

(A) Alignment of *A. nidulans* LreA (AF515628) with homologous proteins of *A. terreus* (CH476606), *A. fumigatus* (XM749933), *N. crassa* (Q01371), *T. atroviride* (AY628431), *Phycomyces blakesleeanus* (1) (DQ229145), and *P. blakesleeanus* (2) (DQ229146).

(B) Alignment of *A. nidulans* LreB (AF082072) with homologous proteins of *A. clavatus* (XM001272120), *A. fumigatus* (XM746470), *A. oryzae* (AP007150), *A. terreus* (XM001212330), *N. crassa* (XM958726), *T. atroviride* (AY628432), and *C. neoformans* (XM570708).

Alignments were done with ClustalW (http://www.ebi.ac.uk/clustalW) and shading with Boxshade 3.21 (http://www.ch.embnet.org/software/BOX_form.html).

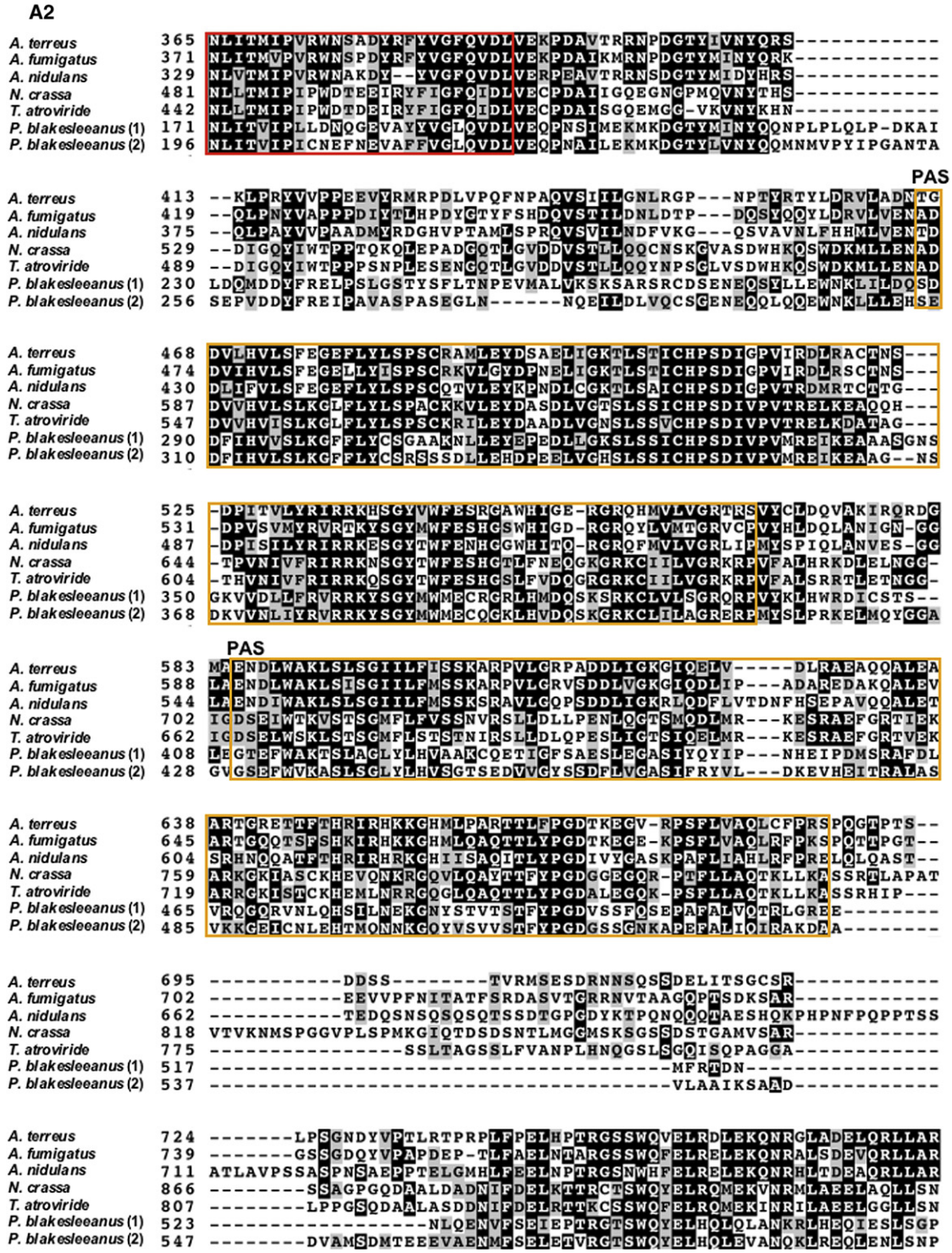

Figure S1 (Continued on next page).

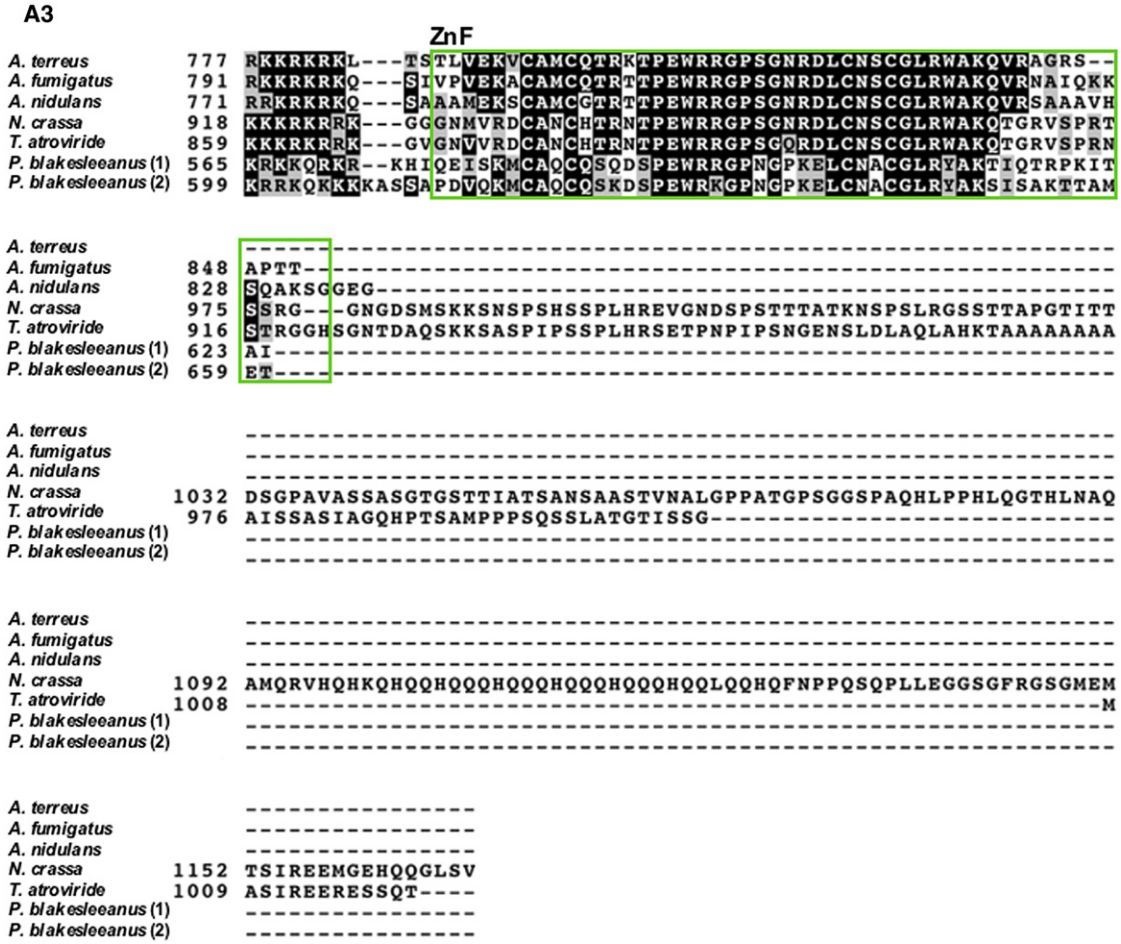

Figure S1 (Continued on next page).

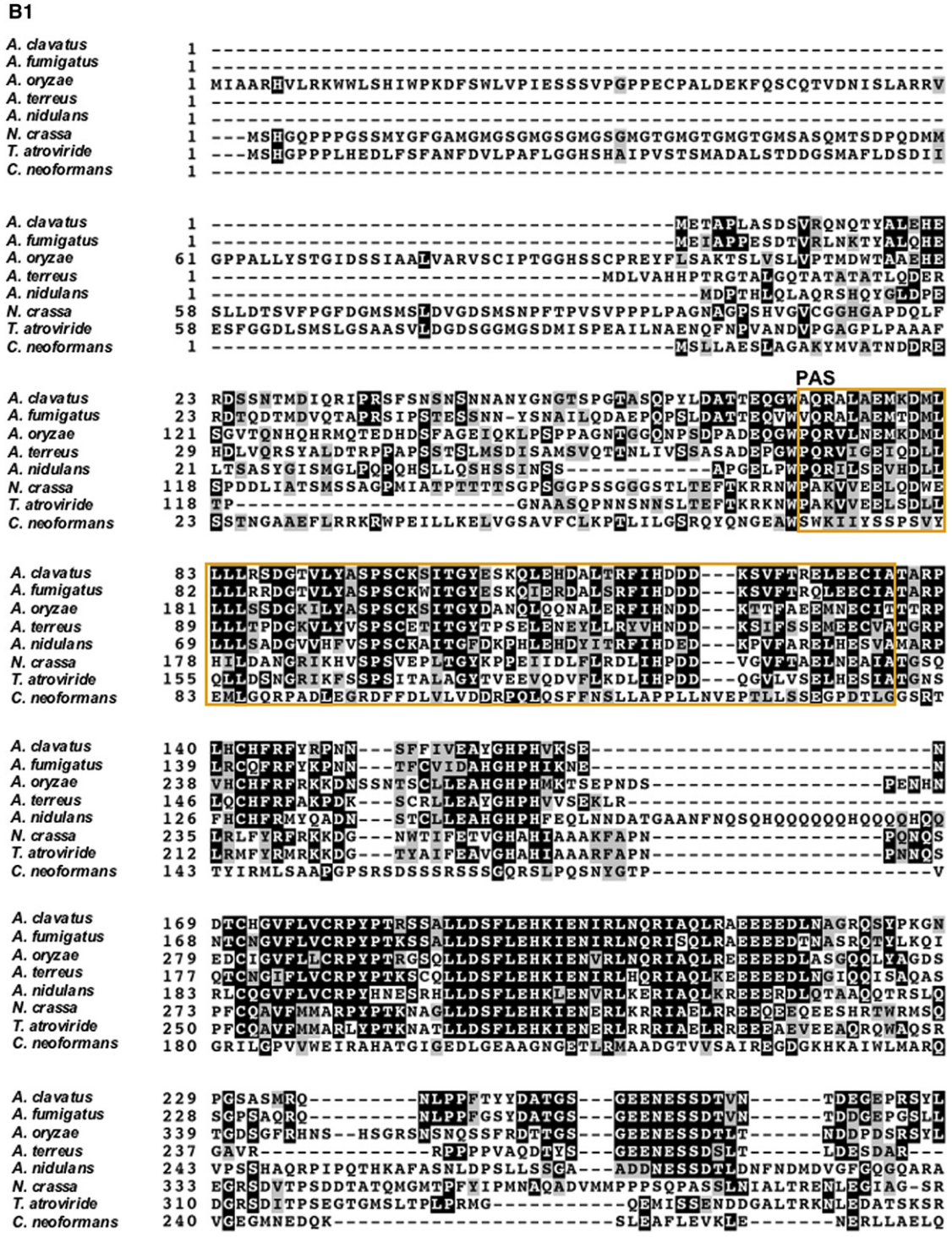

Figure S1 (Continued on next page).

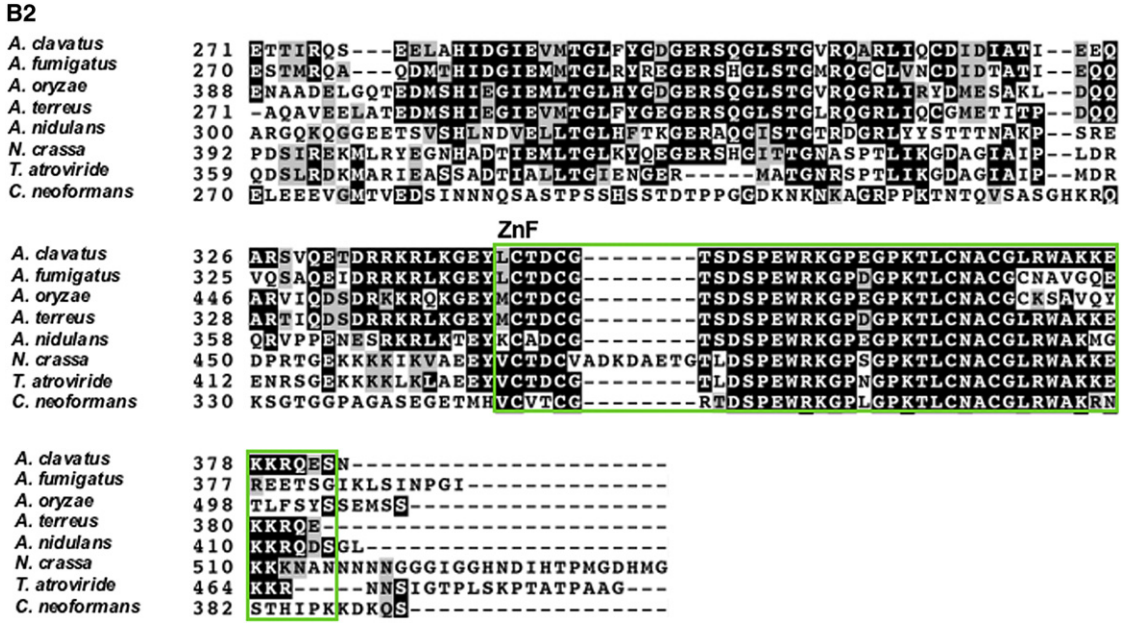

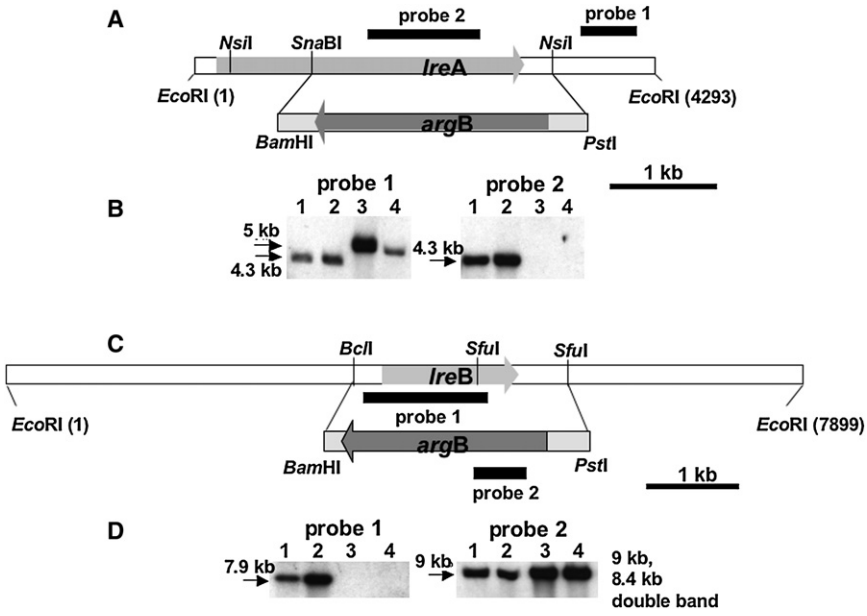

Figure S2. Deletion of *lreA* and *lreB*

(A) Deletion construct for *lreA*.

(B) Southern blot of two wild-type (lane 1, FGSCA4; lane 2, WG335) and two deletion strains (lane 3, LREA13-2; lane 4, LA/V+). Genomic DNA was isolated and restricted with EcoRI. A 0.6 kb fragment was used as probe 1 generated by PCR (primers OW7, OW32), and a 1 kb fragment was used for hybridization in case of probe 2 (primers OW5, OW10).

(C) Deletion construct for *lreB*.

(D) Southern blot of wild-type (lane 1, FGSCA4; lane 2, WG335) and two deletion strains (lane 3, LREB52; lane 4, LB/V+). Genomic DNA was isolated and restricted with EcoRI. A 1.4 kb PCR fragment was used as probe (primers OLR5, OLR6R). As second probe a 0.6 kb fragment was taken for hybridization (primers OARG1, OARG2).

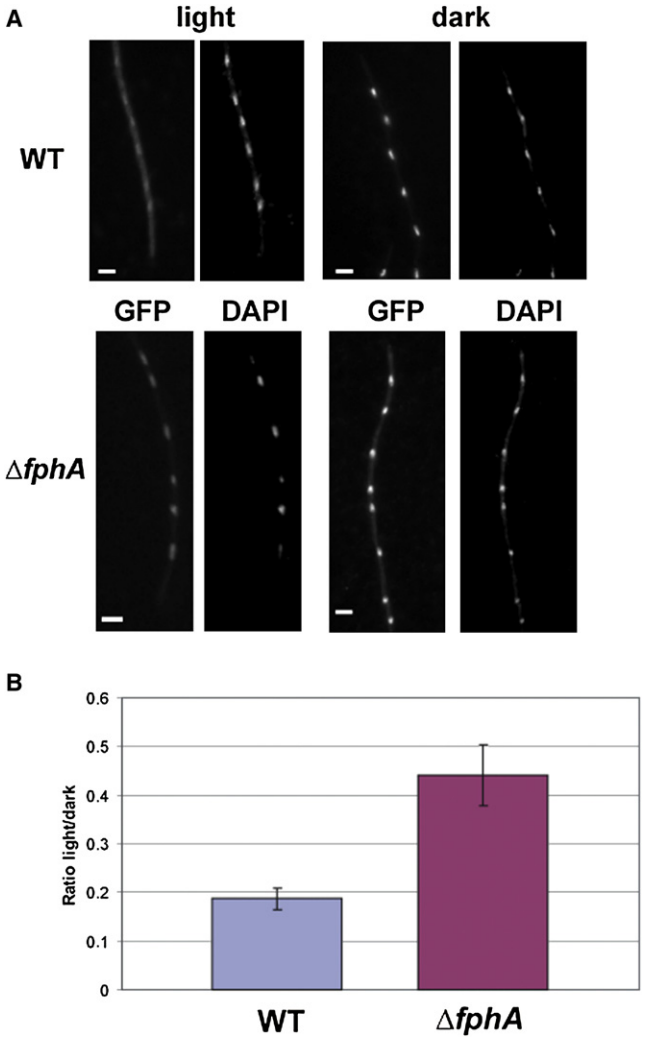

Figure S3. Effect of *fphA* Deletion on Nuclear Concentration of VeA

(A) VeA-GFP localization in the wild-type under light conditions and in the dark (upper row) and in the Δ*fphA* strain (lower row). Nuclear localization was shown by DAPI staining. Hyphae are 3–4 μm in diameter.

(B) Quantification of the accumulation of VeA-GFP in the nucleus. The ratio between the fluorescence intensity of nuclei in the light and in the dark is shown. Error bars represent the standard deviation.

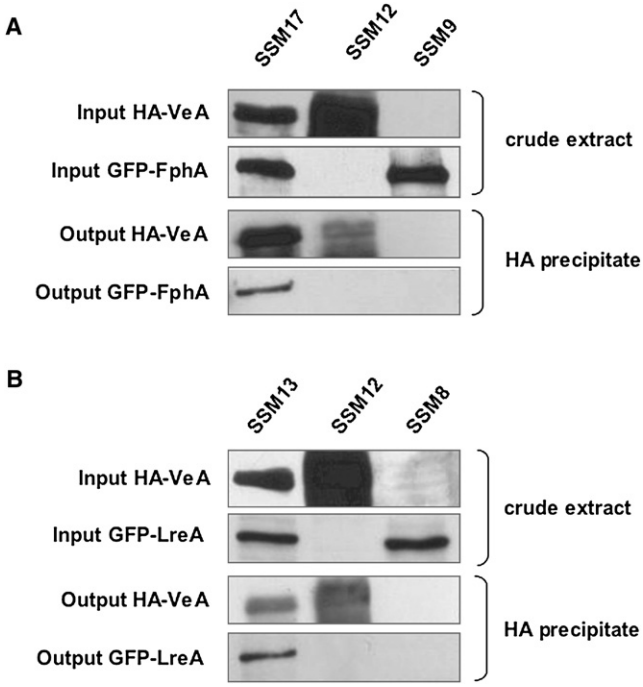

Figure S4. Detection of Protein Interactions by Coimmunoprecipitations

Interaction between VeA and FphA (A) and between VeA and LreA (B). Immunoprecipitations were done with an antibody against the hemeagglutinine epitope of the HA-VeA fusion protein.

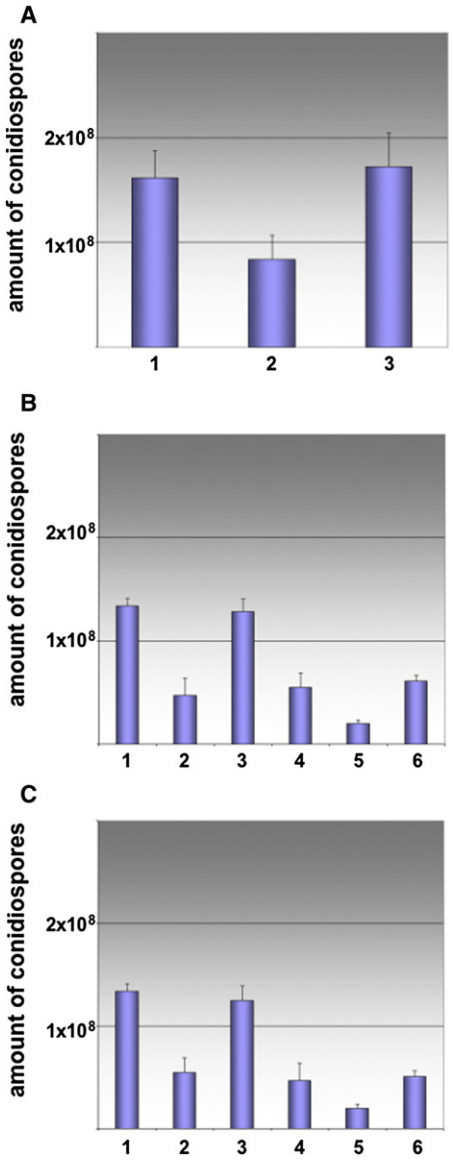

Figure S5. Recomplementation of Light-Receptor Mutants Cultivated under White-Light Illumination

(A) Recomplementation of the Δ*fphA* strain SJP1 with *fphA* expressed under its native promoter. Shown are WT (FGSC A4) (1), SJP1 (2), and SJP22.1 (3).
(B) Recomplementation of several Δ*lreA* mutant strains with *lreA* expressed under the control of the native promoter (pJP33). Shown are SJP1 (1), SJP15G (2), SJP37 (3), SJP13.3 (4), SJP21.3 (5), and SJP39 (6).
(C) Recomplementation of several Δ*lreB* mutant strains with *lreB* containing cosmid plreB65. Shown are SJP1 (1), SJP13.3 (2), SJP52 (3), SJP15G (4), SJP21.3 (5), and SJP51 (6). The inocculation, cultivation, and quantification of conidiospores were done as described in the Experimental Procedures. Error bars represent the standard deviation.

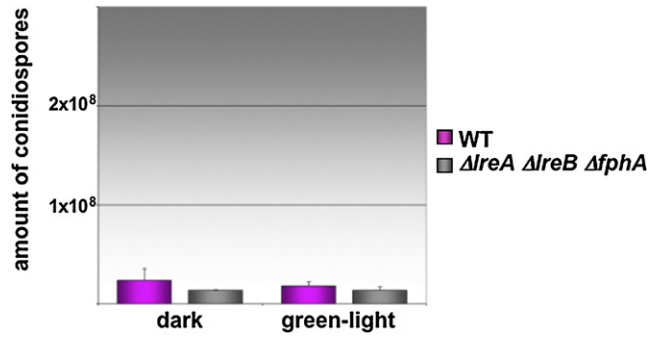

Figure S6. Green-Light Illumination Control

In the wild-type strain FGSCA4 and the triple-knockout strain SJP21.3, green light was not able to induce sporulation. The inocculation, cultivation, and quantification of conidiospores were done as described in the Experimental Procedures. Error bars represent the standard deviation.

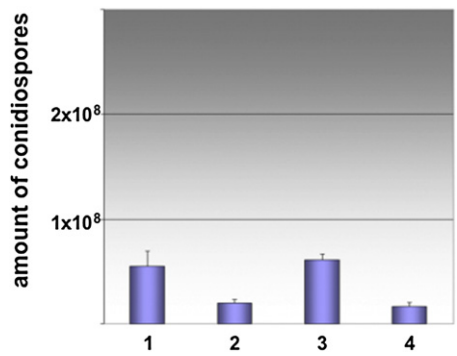

Figure S7. LreAC276A Is Not Functional to Recomplement *lreA* Deletion

Shown are SJP13.3 (1), SJP21.3 (2), SJP39 (3), and SJP98 (4). Strains were inoculated and illuminated with white light as described in the Experimental Procedures. The mutation of the conserved Cys276 residue, which is the putative chromophore-binding site, abolished recomplementation of the *lreA* deletion. Error bars represent the standard deviation.

Table 1. *A. nidulans* Strains Used in This Study

Strain	Genotype	Source
FGSCA4	wild-type	Fungal Genetics Stock Center, Kansas City, Missouri
GR5	*pyrG89; wA3; pyroA4; veA1*	[S7]
SRF200	*pyrG89; ΔargB::trpCΔB; pyroA4; veA1*	[S8]
WG355	*argB; biA1; bgaO; veA1*	[S9]
UC9	*yA2, pabaA1; argB; pyroA4*	L. Yager, University of Philadelphia, Pennsylvania
RSMS3.4A	*pyrG89; pyroA4; veA+; ΔfphA::argB*	This study
RSMS3.4	*pyrG89; pyroA4; veA+*	This study
RSMS2.3A	*ΔfphA::argB; pyroA4; pyrG89; veA+*	This study
TEEAMC8	*ΔfphA::argB; pyroA4; pyrG89; veA::GFP*	This study
TREMD3.4.17	*pyroA4; veA::gfp*	[S6]
SAB6	SRF200 transformed with pAB14 (*alcA::fphA::HA; argB*)	[S4]
SCK5	GR5 transformed with pCK5 (*alcA::GFP::lreB; pyr4*)	This study
SCK6	GR5 transformed with pCK1 (*alcA::YFP-CT:: veA; pyr4*) and pJP4 (*alcA::YFP-NT:: fphA; pyr4*)	This study
SCK9	GR5 transformed with pCK6 (*alcA::GFP:: lreA; pyr4*)	This study
SCK23	GR5 transformed with pCK5 (*alcA::GFP::lreB*; *pyr4*) and pAB14 (*alcA::fphA::HA; argB*)	This study
SCK24	SKV103 transformed with pCK3 (*alcA::YFP-CT:: lreB ;pyr4*) and pCK8 (*alcA::YFP-NT::lreA; pyr4*)	This study
SCK25	SKV103 transformed with pCK3 (*alcA::YFP-CT::lreB ; pyr4*) and pJP4 (*alcA:: YFP-NT::fphA; pyr4*)	This study
SCK26	SKV103 transformed with pJP4 (*alcA::YFP-NT:: fphA; pyr4*) and pCK7 (*alcA::YFP-CT::lreA; pyr4*)	This study
SCK27	SKV103 transformed with pCK8 (*alcA::YFP-NT::lreA; pyr4*) and pCK1 (*alcA::YFP-CT::veA; pyr4*)	This study
SCK28	SKV103 transformed with pCK1 (*alcA::YFP-CT::veA; pyr4*) and pCK4 (*alcA::YFP-NT::lreB; pyr4*)	This study
SCK29	SKV103 transformed with pCK7 (*alcA::YFP-CT::lreA; pyr4*) and pCK8 (*alcA::YFP-NT::lreA; pyr4*)	This study
SCK30	SKV103 transformed with pCK3 (*alcA::YFP-CT::lreB; pyr4*) and pCK4 (*alcA::YFP-NT::lreB;pyr4*)	This study
SCK31	SKV103 transformed with pCK1 (*alcA::YFP-CT::veA; pyr4*) and pCK2 (*alcA::YFP-NT::veA; pyr4*)	This study
SSM7	SRF200 transformed with pAB14 (*alcA::fphA::HA; argB*) and pCK6 (*alcA::GFP::lreA; pyr4*)	This study
SSM8	GR5 transformed with pCK6 (*alcA::GFP::lreA; pyr4*)	This study
SSM9	GR5 transformed with pJP2 (*alcA::GFP::fphA*)	This study
SSM12	GR5 transformed with pSM17 (*alcA::HA::veA*)	This study
SSM13	GR5 transformed with pCK6 (*alcA::GFP::lreA*) and pSM17 (*alcA::HA::veA*)	This study
SSM17	GR5 transformed with pJP2 (*alcA::GFP::fphA*) and pSM17 (*alcA::HA::veA*)	This study
LREA13-2	*biA1; ΔlreA::argB; argB; bgaO; veA1*	This study
LREB52	*biA1; ΔlreB::argB; bgaO; veA1*	This study
LAV+	*biA1; ΔlreA::argB; veA+*	This study
LBV+	*biA1; ΔlreB::argB; pyroA4; veA+*	This study
SJP1	*pyrG89; ΔargB::trpCΔB; pyroA4; ΔfphA::argB; veA+*	This study
SJP13.3	cross between LBV+ and SJP1—*biA1*; *ΔlreB::argB; ΔargB:trpCΔB; pyroA4; ΔfphA::argB; veA+*	This study
SJP15G	cross between LAV+ and SJP1—*pyrG89; ΔargB:trpCΔB; pyroA4; ΔlreA::argB, ΔfphA::argB; veA+*	This study
SJP21.3	cross between SJP15G and SJP13.3—*pyrG89; ΔlreB::argB; ΔargB:trpCΔB; pyroA4; ΔlreA::argB, ΔfphA::argB; veA+*	This study
SJP22.1	SJP1 transformed with pJP19 (*fphA with native promoter, pyr4*)	This study
SJP32	GR5 transformed with pJP52 (*alcA::YFP-CT:: fphAC195A*) and pCK4 (*alcA::YFP-NT::lreB, pyr4*)	This study
SJP33	GR5 transformed with pJP52 (*alcA::YFP-CT::fphAC195A*) and pCK2 (*alcA::YFP-NT::veA, pyr4*)	This study
SJP34	GR5 transformed with pJP37 (*alcA::YFP-NT::fphAΔRPKK; pyr4*) and pCK3 (*alcA::YFP-CT:: lreB*)	This study
SJP35	GR5 transformed with pJP39 (*alcA::YFP-NT:: fphAΔRRRK; pyr4*) and pCK3 (*alcA::YFP-CT:: lreB*)	This study
SJP37	SJP15G transformed with pJP33 and pRG1 (*lreA with native promoter*)	This study

Table 1. *Continued*

Strain	Genotype	Source
SJP39	SJP21.3 transformed with pJP33 and pRG1 (*lreA with native promoter*)	This study
SJP43	GR5 transformed with pJP48 (*alcA::YFP-NT::fphAΔRPKKΔRRRK; pyr4*) and pCK3 (*alcA::YFP-CT::lreB*)	This study
SJP44	GR5 transformed with pJP4 (*alcA::YFP-NT:: fphA; pyr4*) and pJP52 (*alcA::YFP-CT:: fphAC195A*)	This study
SJP51	SJP21.3 transformed with plreB65 and pRG1 (*lreB with native promoter*)	This study
SJP52	SJP13.3 transformed with plreB65 and pRG1 (*lreB with native promoter*)	This study
SJP98	SJP21.3 transformed with pJP75 and pRG1 (*lreAC276A with native promoter*)	This study

Table 2. Plasmids Used in This Study

Plasmids	Construction	Source
pCR2.1-TOPO	cloning vector	Invitrogen (NV Leek, The Netherlands)
pGEM-T	cloning vector	Promega (Mannheim)
pBS-KS	cloning vector	Stratagene (Heidelberg)
pMCB17apx	for fusion of proteins with GFP under control of alcA(p)	V.P. Efimov, Piscataway, New Jersey
pJP2	*alcA::GFP::fphA; pyr4*	[S4]
pJP4	*alcA::YFP-NT::fphA; pyr4*	[S4]
pJP5	*alcA::YFP-CT::fphA; pyr4*	This study
pJP7.1	*alcA::gfp::fphAC195A of fphA, pyr-4*	This study
pJP19	*fphA (native promoter), pyr4*	This study
pJP33	*lreA (native promoter), pyr4*	This study
pJP37	*alcA::YFP-NT::fphAΔRPKK; pyr4*	This study
pJP39	*alcA::YFP-NT::fphAΔRRRK; pyr4*	This study
pJP48	*alcA::YFP-NT::fphAΔRPKK ΔRRRK; pyr4*	This study
pJP52	*alcA::YFP-CT::fphAC195A*	This study
pJP75	*lreAC276A (native promoter), pyr4*	This study
pILJ16	*argB*-containing plasmid	[S10]
W16/G02	*lreA*-containing cosmid	This study
pL1E5	*lreA*-containing plasmid	This study
W21/A03	*lreB*-containing cosmid	This study
pLREB65	*lreB*-containing plasmid	This study
pLREA/KO	*lreA::argB*	This study
pLREB/KO	*lreB::argB*	This study
pCK1	*alcA::YFP-CT::veA, pyr4*	This study
pCK2	*alcA::YFP-NT::veA, pyr4*	This study
pCK3	*alcA::YFP-CT::lreB, pyr4*	This study
pCK4	*alcA::YFP-NT::lreB, pyr4*	This study
pCK5	*alcA::GFP::lreB, pyr4*	This study
pCK6	*alcA::GFP::lreA, pyr4*	This study
pCK7	*alcA::YFP-CT::lreA, pyr4*	This study
pCK8	*alcA::YFP-NT::lreA, pyr4*	This study
pI4	*pyroA*	[S11]
pRG1	*pyr4*	[S7]